Synthesis and photoluminescence properties of $Ba_2Y_3(SiO_4)_3F:Tm^{3+}$ blue-emitting fluorosilicate phosphors

Junhui Yang[1,2], Huanyou Wang[1,2], Jinhua Liu[1,2], Jun Chen[1,2], Fanhua Zeng[1,2], Bin Deng*[1,2]

[1]College of Chemistry & Biology and Environmental Engineering, Xiangnan University, Chenzhou 423043, Hunan, P. R. China
[2]Hunan Provincial Key Laboratory of Xiangnan Rare-Precious Metals Compounds Research and Application, Chenzhou 423043, Hunan, P. R. China

Abstract. Various novel $Ba_2Y_3(SiO_4)_3F:Tm^{3+}$ blue-emitting fluorosilicate materials were achieved via solid-state synthesis. The structure and phase purity of prepared $Ba_2Y_3(SiO_4)_3F:xTm^{3+}$ (x = 0.001-0.10 mol) were examined by X-ray powder diffraction. The surface morphology of $Ba_2Y_3(SiO_4)_3F:0.01Tm^{3+}$ was studied by scanning electron microscopy. Photoluminescence properties were systematically explored under the monitoring emission (λ_{em} = 468 nm) and excitation (λ_{ex} = 302 nm) spectra. The optimum mole ratio of as-synthesized phosphors was 0.01 mol. The concentration quenching mechanism in the $Ba_2Y_3(SiO_4)_3F$ host was due to electric multipole interaction. Particularly, the chromaticity coordinates (0.1334, 0.0474) of $Ba_2Y_3(SiO_4)_3F:0.01Tm^{3+}$ are near to those of the commercial $BaMgAl_{10}O_{17}:Eu^{2+}$. These results validated the $Ba_2Y_3(SiO_4)_3F:Tm^{3+}$ fluorosilicate phosphor can be used as a good blue-emitting candidate for W-LEDs.

1 Introduction

Solid-state lighting devices have been made great progress in the development of society. The devices are commonly fabricated by using light-emitting-diodes (LEDs) and phosphors. Because LEDs have virtues of energy-saving, environmental friendliness and high efficiency [1-6]. Currently, W-LEDs are realized by combining the output from the blue LED chip with the yellow-emitting phosphor $Y_3Al_5O_{12}:Ce^{3+}$ phosphor. Unfortunately, these products lacked red composition, which leads to lower color rendering index and high correlated color temperature [7]. Hence, an alternative method was proposed by combining tricolor (RGB) phosphors coated onto a near-UV (NUV) chip [8, 9]. It is imperative to fabricate a novel blue-emitting phosphor with effective absorption in the near-UV region.

There are many kinds of phosphors those have been reported. Rare-earth ions doped silicates have arisen extensive interest due to excellent chemical and physical stability, such as $BaY_2Si_3O_{10}:Tm^{3+}$, Dy^{3+}, $K_4CaSi_3O_9:Eu^{3+}$, and $RbNa_3(Li_3SiO_4)_4:Eu^{2+}$ [10-12]. Tm^{3+} is widely used as an efficient blue light emitting center [13]. $CaHfO_3:Tm^{3+}$, $Li_3Gd_3Te_2O_{12}:Tm^{3+}$, and $CaBi_4Ti_4O_{15}:Tm^{3+},Yb^{3+}$, etc., many alternative Tm^{3+}-doped phosphors have been reported [14-16]. In this work, Tm^{3+}-doped $Ba_2Y_3(SiO_4)_3F$ blue-emitting phosphor for W-LEDs has been synthesized by solid-state reaction. The powder X-ray diffraction (XRD) of the samples were taken and discussed in this paper. The surface morphology, the photoluminescence (PLE) properties, the emission PL spectra, concentration quenching mechanism, and CIE coordinates were investigated in depth.

2 Experimental

The $Ba_2Y_{3(1-x)}Tm_{3x}(SiO_4)_3F$ powders were achieved through solid-phase synthesis method. $BaCO_3$ (analytical reagent), SiO_2 (nanopowder, 99.5%), Y_2O_3 (analytical reagent), BaF_2 (analytical reagent), Tm_2O_3 (99.99%) were taken as starting materials. First, the mixture was ground thoroughly for 15 minutes and set into proper size crucibles. Then, the mixture was calcined in air at 600℃ for one hour, and further sintered at 1200 °C for 5 h. Finally, after the muffle furnace cooled down to room temperature, the products were ground for luminescence characterization. The structural properties of phosphor were measured by XRD through a Bruker D2 PHASER X-ray diffractometer with Cu Kα radiation source (λ = 0.15405 nm) operated at 40 kV with results between the range of 2θ = 15°−70°. The surface morphology was studied via a JEOL JSM-6490 emission scanning electron microscopy (SEM). The photoluminescence spectra of all the samples were characterized by F4600 spectrometer (Hitachi)

* Corresponding author: dengbinxnu@163.com

3 Results and discussion

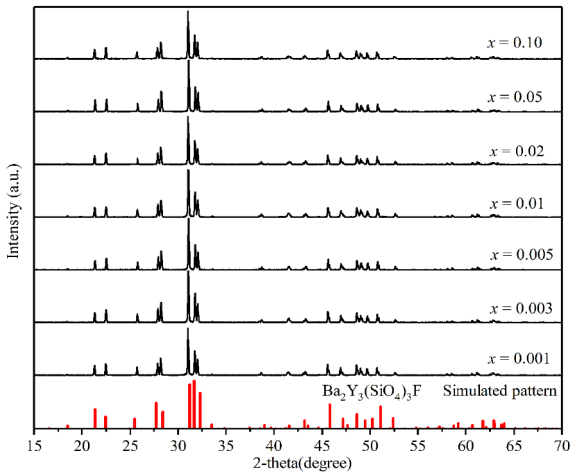

Fig. 1. XRD patterns of the $Ba_2Y_3(SiO_4)_3F$:xTm^{3+} phosphors (x = 0.001, 0.003, 0.005, 0.01, 0.02, 0.05, and 0.10).

Figure 1 presents the representative XRD patterns of $Ba_2Y_{3(1-x)}Tm_{3x}(SiO_4)_3F$ (x = 0.001, 0.003, 0.005, 0.01, 0.02, 0.05, and 0.10) phosphors. Obviously, with the increase of Tm^{3+} dopant concentration, all the diffraction peaks were in accordance with the simulated patterns generated by the structural parameters of $Ba_2Y_3(SiO_4)_3F$ [17, 18]. It indicated the small amount of Tm^{3+} ions does not evidently influence the crystal structure of $Ba_2Y_3(SiO_4)_3F$. The unit cell lattice parameters, for the composition of $Ba_2Y_3(SiO_4)_3F$:$0.01Tm^{3+}$, are $a = b$ = 9.696 Å, c = 6.913 Å and V = 562.86 Å^3, respectively. Hence, the ionic radii of the Y^{3+} and Tm^{3+} ions are approximate corresponding to 1.019 Å and 0.994 Å (coordination number, CN = 8), respectively [19]. Obviously, a small amount of Y^{3+} ions can be readily replaced by Tm^{3+} ions in the $Ba_2Y_3(SiO_4)_3F$ host lattice.

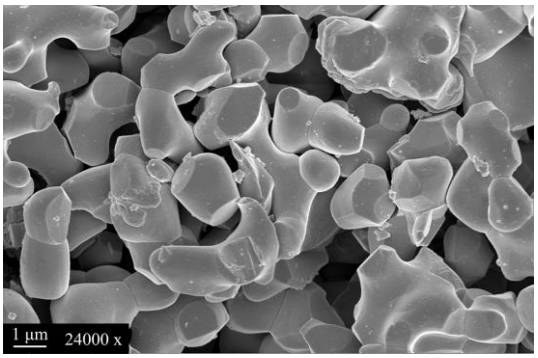

Fig. 2. SEM micrograph of a representative of $Ba_2Y_3(SiO_4)_3F$:$0.01Tm^{3+}$ sample.

Generally, the mean size of commercial phosphor particles was in the range of 5−10 μm. Figure 2 presents the SEM micrograph of a representative of $Ba_2Y_3(SiO_4)_3F$:$0.01Tm^{3+}$ sample. The particle sizes were distributed in the range of a few microns to a few hundred microns. The shape of particles were irregular and non-uniform because of the annealing process under high temperature.

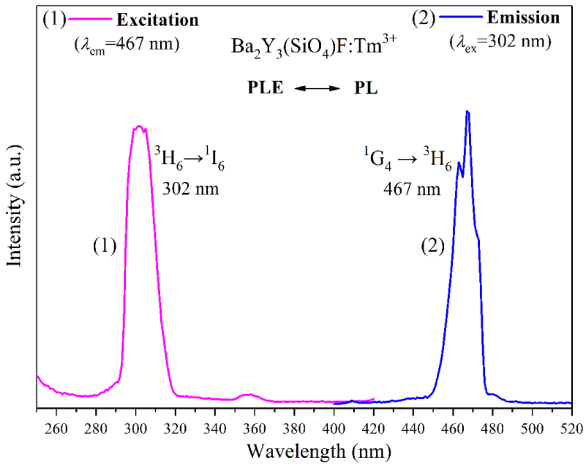

Fig. 3. Excitation spectrum (λ_{em} = 468 nm) and emission spectrum (λ_{ex} = 302 nm) of $Ba_2Y_3(SiO_4)_3F$:$0.01Tm^{3+}$ phosphor.

The excitation spectrum of representative sample $Ba_2Y_3(SiO_4)_3F$:$0.01Tm^{3+}$ is monitored at 467 nm and shown in Figure 3 curve (1). A peak in the excitation spectrum at 302 nm is assigned to the typical 4*f*–4*f* transition of $^3H_6 \rightarrow {}^1I_6$ of Tm^{3+}. Figure 3 curve (2) displays the emission spectrum of $Ba_2Y_3(SiO_4)_3F$:$0.01Tm^{3+}$ at near-UV light λ_{ex} = 302 nm. The main emission band at 467 nm due to the electronic dipole transition of $^1G_4 \rightarrow {}^3H_6$ of Tm^{3+} [20]. Importantly, the emission peaks situated in the blue region suggested that $Ba_2Y_3(SiO_4)_3F$:Tm^{3+} can be promising blue emitting phosphors.

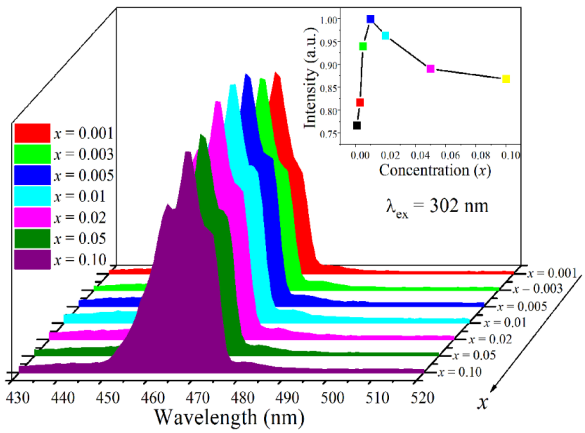

Fig. 4. The PL spectra (λ_{ex} = 302 nm) of $Ba_2Y_{3(1-x)}Tm_{3x}(SiO_4)_3F$ (x = 0.001, 0.003, 0.005, 0.01, 0.02, 0.05, and 0.10) phosphors. The upper inset showed the influence of Tm^{3+} icon with different concentrations.

The PL spectra of $Ba_2Y_{3(1-x)}Tm_{3x}(SiO_4)_3F$ (x = 0.001, 0.003, 0.005, 0.01, 0.02, 0.05, and 0.10) as with different Tm^{3+} ions content are presented in Figure 4. It is obvious that all the emission spectra have similar shape profiles with the increasing concentration. When the doping Tm^{3+} concentration in $Ba_2Y_{3(1-x)}Tm_{3x}(SiO_4)_3F$ was x = 0.01 mol, the emission intensity of the sample reached the most intense. Subsequently, exceeding 0.01 mol, the emission intensities of Tm^{3+} began to decrease gradually owing to concentration quenching phenomenon. It is induced through the resonant energy transfer.

The critical transfer distance (R_c) was proposed by Blasse for analyzing the energy transfer mechanism, and the value can be estimated by this equation (1) [21, 22]:

$$R_c \approx 2\left(\frac{3V}{4\pi\ x_c N}\right)^{1/3} \qquad (1)$$

here V (562.86 Å^3) referred to the cell volume, X_c (0.01) represented the best doping concentration, and N (2) was the number of substitutable cations in a unit cell, the critical transfer distance R_c was estimated to be 37 Å, much higher than that of exchange interaction distance (5.0 Å). Therefore, the electric multipole interactions between Tm^{3+} ions will be responsible for the concentration quenching phenomenon.

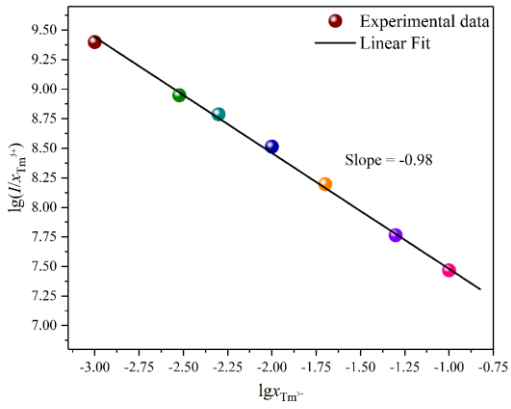

Fig. 5. Dependence of lg$x$ on lg(I/x) of $Ba_2Y_3(SiO_4)_3F:Tm^{3+}$ phosphors.

Furthermore, the following equation was used to evaluate the specific type of interaction mechanism in the energy transfer process of Tm^{3+} ions according to the theory of Dexter [23] :

$$\frac{I}{x} = K\left[1+\beta\left(x\right)^{Q/3}\right]^{-1} \qquad (2)$$

Here, Q is constant at 3, 6, 8, and 10. They represent different energy transfer interactions, such as the nearest-neighbor ions (Q=3), electric dipole-dipole (Q=6), dipole-quadrupole (Q=8), or quadrupole-quadrupole (Q=10) interactions, respectively [24, 25]. x stood for the activator concentration, K and β were constants at the same excitation condition. Figure 5 illustrates the linear plot. The slope parameter of the line was found to be −0.98. The Q value was fitted to 2.94, which approaches 3, indicating that the interaction between the nearest neighbor ions was the major reason for the concentration quenching of $Ba_2Y_3(SiO_4)_3F:Tm^{3+}$ phosphors [26, 27].

The CIE 1931 chromaticity coordinates are important parameters for evaluating the luminescent properties of materials [28-30]. The CIE chromaticity diagram of $Ba_2Y_3(SiO_4)_3F:xTm^{3+}$ (x = 0.001-0.10 mol) under 302 nm excitation were displayed in Figure 6 with the red stars. The CIE color coordinates of $Ba_2Y_3(SiO_4)_3F:0.01Tm^{3+}$ (x = 0.1343, y = 0.0516) were close to the standard blue position of the $BaMgAl_{10}O_{17}:Eu^{2+}$. These red stars were near the edge of the CIE gamut indicated the high blue color purity of $Ba_2Y_3(SiO_4)_3F:Tm^{3+}$ phosphors.

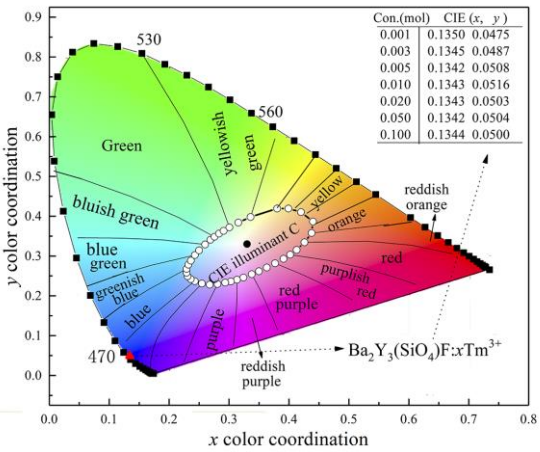

Fig. 6. CIE chromaticity diagram of the $Ba_2Y_3(SiO_4)_3F:Tm^{3+}$ phosphors

4 Conclusions

The solid-state reaction method was successfully used to prepare the $Ba_2Y_3(SiO_4)_3F:Tm^{3+}$ phosphors. When excited at 302 nm, the $Ba_2Y_3(SiO_4)_3F:Tm^{3+}$ phosphors presented main emission peaks at 467 nm. The highest relative luminescence intensity was achieved at 0.01 mol doping level. After that, concentration quenching occurred due to the interaction of the nearest-neighbor ion. The critical distance was 37 Å related to concentration quenching. The CIE color coordinate were close to the standard blue position. These indicated that the phosphor can emit blue light with high purity. In conclusion, the $Ba_2Y_3(SiO_4)_3F:Tm^{3+}$ phosphor is a promising blue-emitting candidate for W-LEDs.

Acknowledgments

This project was financially supported by the Construction Program of the key discipline in Hunan Province, the Projects of the Education Department of Hunan Province (No.18A465), and Science and Technology Plan Project of Chenzhou city (jsyf2017014). The authors declared that there were no conflicts of interest related to this article.

References

1. R. Yu, H.M. Noh, B.K. Moon, B.C. Choi, J.H. Jeong, K. Jang, S.S. Yi, J.K. Jang, J. Alloys Compd. **576**, 236 (2013)
2. G. Zhu, Y. Huang, C. Wang, L. Lu, T. Sun, M. Wang, Y. Tang, D. Shan, S. Wen, J. Zhu, Spectrochim. Acta, Part A **210**, 105 (2019)
3. B. Yang, J. Xu, H.-L. Zhu, Free Radical Biol. Med. **145**, 42 (2019)
4. Z.D. Wang Yurong, Wang Yang, Ye Hao, Yao Wei, Ding Ying, Gu Haiying, Feng Xia, Li Ling, Dai Hong, Chinese J. Org. Chem. **39**, 2053 (2019)
5. Y. Wang, Y. Cai, L. Cao, M. Cen, Y. Chen, R. Zhang, T. Chen, H. Dai, L. Hu, Y. Yao, Chem. Commun. **55**, 10132 (2019)

6. Y. Tang, Y. Huang, Y. Chen, L. Lu, C. Wang, T. Sun, M. Wang, G. Zhu, Y. Yang, L. Zhang, J. Zhu, Spectrochim. Acta, Part A **218**, 359 (2019)
7. Z. Xia, Z. Xu, M. Chen, Q. Liu, Dalton Trans. **45**, 11214 (2016)
8. R. Yu, C. Wang, J. Chen, Y. Wu, H. Li, H. Ma, ECS J. Solid State Sci. Technol. **3**, R33 (2014)
9. R. Li, S. Wang, Q. Li, H. Lan, S. Xiao, Y. Li, R. Tan, T. Yi, Dyes Pigm. **137**, 111 (2017)
10. J. Zhou, Z. Xia, Opt. Mater. **53**, 116 (2016)
11. H. Liao, M. Zhao, M.S. Molokeev, Q. Liu, Z. Xia, Angew. Chem. **130**, 11902 (2018)
12. L. Han, S. Xie, M. Wang, T. Sun, Q. Liu, G. Jiang, Y. Shi, Y. Tang, Mater. Lett. **234**, 241 (2019)
13. Y. Li, J. Zheng, Z. Li, X. Yang, J. Chen, C. Chen, Optik **169**, 257 (2018)
14. H. Fukushima, D. Nakauchi, T. Kato, N. Kawaguchi, T. Yanagida, Radiat. Meas. **133**, (2020)
15. B. Deng, C.S. Zhou, H. Liu, J. Chen, Mater. Sci. Forum **921**, 111 (2018)
16. T. Fu, X. Wang, H. Ye, Y. Li, X. Yao, J. Electron. Mater. **49**, 5047 (2020)
17. R. Yu, N. Xue, T. Wang, Z. Zhao, J. Wang, Z. Hei, M. Li, H.M. Noh, J.H. Jeong, Ceram. Int. **41**, 6030 (2015)
18. B. Deng, J. Chen, H. Liu, C.-s. Zhou, J. Mater. Sci.: Mater. Electron. **30**, 7507 (2019)
19. R.D. Shannon, Acta Crystallogr., Sect. A: Found. Crystallogr. **A32**, 751 (1976)
20. B. Deng, J. Chen, C.-s. Zhou, H. Liu, Optik **202**, 163658 (2020)
21. G. Blasse, B.C. Grabmaier, Springer-Verlag, Berlin, Heidelberg 46 (1994)
22. W. Yang, C. Liu, S. Lu, J. Du, Q. Gao, R. Zhang, Y. Liu, C. Yang, J. Mater. Chem. C **6**, 290 (2018)
23. L.G. Van Uitert, J. Electrochem. Soc. **114**, 1048 (1967)
24. L. Zhang, Y. Xie, X. Geng, B. Deng, H. Geng, R. Yu, J. Lumin. **225**, 117365 (2020)
25. L. Zhang, J. Che, Y. Ma, J. Wang, R. Kang, B. Deng, R. Yu, H. Geng, J. Lumin. **225**, 117374 (2020)
26. Y. Chen, X. Li, N. Li, Y. Quan, Y. Cheng, Y. Tang, Mater.Chem.Front. **3**, 867 (2019)
27. Q. Zhao, G.H. Tao, C.W. Ge, Y. Cai, Q.C. Qiao, X.P. Jia, Spectrosc. Lett. **51**, 216 (2018)
28. S. Xu, Y. Liu, H. Yang, K. Zhao, J. Li, A. Deng, Anal. Chim. Acta **964**, 150 (2017)
29. J. Shen, S. Shang, X. Chen, D. Wang, Y. Cai, Sens. Actuators, B **248**, 92 (2017)
30. Y. Jin, C. Shi, X. Li, Y. Wang, F. Wang, M. Ge, Dyes Pigm. **139**, 693 (2017)